

HIGH-IMPEDANCE FAULT DETECTION TECHNOLOGY BASED ON TRANSIENT INFORMATION IN A RESONANT GROUNDING SYSTEM

Tian You LI
State Grid Fujian Electric Power
Company Limited – China
ltyxm@163.net

Yong Duan XUE
China University of Petroleum (East
China) – China
xueyd70@126.com

Bing Yin XU
Shandong University of
technology–China
xuby@vip.163.com

ABSTRACT

High-impedance faults (HIFs) occur frequently in resonant grounding systems and are difficult to detect. Thus, an effective HIF feeder identification technology is urgently in demand. An HIF equivalent circuit in a resonant grounding system is established. The magnitude and phase relationships of transient zero-sequence currents among the faulty feeder, healthy feeders, detection points and fault point, as well as the relationships between their projection coefficients with respect to the transient zero-sequence voltage are analysed. A novel HIF detection method based on the comparison of the magnitude and polarity of the transient zero-sequence current's projection coefficient is proposed. The accuracy of the proposed method is verified by simulations and field data.

INTRODUCTION

In China and continental Europe, resonant grounding systems exist largely in medium-voltage distribution networks. Because of the natural environment, low overhead line and other factors, single-phase HIFs frequently occur when the conductors break and fall to the ground or when the conductors touch the tree branches [1]. HIFs account for 12% of all grounded faults in France [2]. HIF detection in a resonant grounding system is still a considerable challenge because the fault current can decrease to less than 2 A and the fault point is unstable.

HIF detection methods for a resonant grounding system are less established. Reference [3] uses the phasor relationship of the three-phase current variation before and after the fault to calculate the admittance to ground; the faulty feeder has the largest admittance to ground. However, the three-phase currents are influenced by the inconsistency of the Current Transformers (CTs) of the three phases, which affects the practical application performance. Reference [4] uses the active power component of the zero-sequence power frequency current to determine the faulty feeder in the HIF. The HIF active current is small and influenced by the transmission error of CT and potential transformer (PT), which will also affect the practical application performance. References [5],[6] perform the integration of the zero-sequence current of all feeders from the time when the zero-sequence voltage is zero up to the actual trigger time. The

faulty feeder is the one in which the integration of the zero-sequence current is no longer proportional to the zero sequence voltage. The practical application performance is good, but the integration accumulates error easily, and the linear relation and nonlinear relation judgment are strongly influenced by the subjective factors. Thus, the algorithm must be further improved. In addition, the study of HIF location is relatively less, fresh rare to relevant results.

In this paper, an HIF equivalent circuit is established in a resonant grounding system. The magnitude and phase relationships of transient currents among the faulty feeder, healthy feeders, detection points and fault points, as well as the relationships between their projection coefficient with respect to the transient voltage are analyzed. A novel transient approach for a resonant grounding system is proposed. The new method uses the projection coefficient of transient current with respect to transient voltage to detect the HIF. The feasibility of the proposed method are verified by simulations and field data.

IDENTIFICATION METHOD OF HIF IN RESONANT GROUNDING SYSTEM

Analysis of the transient electric quantities in HIF

Based on reference [7], the equivalent circuit which is suitable for the analysis of HIF detection in resonant grounding systems can be established and is shown in Fig.1. The system has n feeders (the faulty feeder is named feeder n). In Fig.1, u_f is the virtual voltage source at the fault point, u_c is the zero-sequence voltage, L_p is 3 times of the inductance of Petersen coil, R is three times as much as the transition resistance at the fault point. i_{Lp} and i_f are the zero-sequence current of the Petersen coil and the fault point, respectively. In the upstream part of the fault point, C_j ($j = 1, 2, \dots, j, \dots, n-1$) is the zero-sequence distributed capacitance to the ground for each healthy feeder, i_j is the zero-sequence current for every healthy feeder, i_n is the zero-sequence current for faulty feeder. Assuming that there are m detection points (Q_m) in the faulty feeder, the faulty feeder can be divided into m sections. C_{nk} ($k= 1, 2, \dots, i, m$) is the zero-sequence distributed capacitance to the ground for the first k section, i_{Qk} is the zero-sequence current for the first k detection point, then $i_n = i_{Q1}$ is got; $C_n = \sum_{k=1}^m C_{nk}$ is the

zero-sequence capacitance to the ground for faulty feeder, $C_{\Sigma} = \sum_{j=1}^{n-1} C_j + C_n$ is system's total zero-sequence capacitance to the ground.

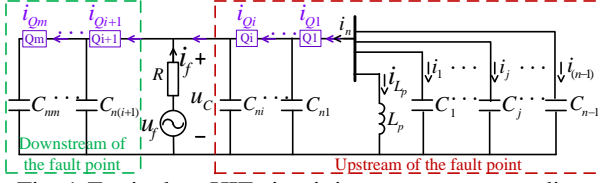


Fig. 1-Equivalent HIF circuit in a resonant grounding system with n feeders

According to the Fig.1, the second-order non-homogeneous linear differential equation is established:

$$R(C_{\Sigma} \frac{d^2 i_{L_p}}{dt^2} + i_{L_p}) + L_p \frac{di_{L_p}}{dt} = u_f(t) = U_m \sin(\omega_0 t + \theta) \quad (1)$$

U_m is the peak value of virtual voltage source at the fault point, θ is the fault inception angle.

When R is in the following range:

$$R > \frac{1}{2} \sqrt{\frac{L_p}{C_{\Sigma}}} \quad (2)$$

the system is in the under-damping state. The under-damping state is the main state of an HIF.

The transient current at the fault point (transient zero-sequence current component is referred to as the transient current, the same below) can be expressed as

$$i_{f-T} = -\frac{L_p(A_2\omega_f - \delta A_1)}{R} e^{-\delta t} \cos(\omega_f t) - \frac{L_p(-A_1\omega_f - \delta A_2)}{R} e^{-\delta t} \sin(\omega_f t) \quad (3)$$

where

$$A_1 = -B \sin \varphi; A_2 = \frac{-\delta B \sin \varphi - \omega_0 B \cos \varphi}{\omega_f} \quad (4)$$

$$\delta = \frac{1}{2RC_{\Sigma}}; \omega_f = \sqrt{\frac{1}{L_p C_{\Sigma}} - \left(\frac{1}{2RC_{\Sigma}}\right)^2} \quad (5)$$

The transient voltage of the bus can be expressed as

$$u_{C-T} = L_p(-A_1\omega_f - \delta A_2)e^{-\delta t} \sin(\omega_f t) + L_p(A_2\omega_f - \delta A_1)e^{-\delta t} \cos(\omega_f t) \quad (6)$$

The transient current of healthy feeders, which is equal to its capacitance ground transient current, can be expressed as

$$i_{j-T} = L_p C_j (\delta^2 A_1 - A_1 \omega_f^2 - 2\delta A_2 \omega_f) e^{-\delta t} \cos(\omega_f t) + L_p C_j (\delta^2 A_2 - A_2 \omega_f^2 + 2\delta A_1 \omega_f) e^{-\delta t} \sin(\omega_f t) \quad (7)$$

The transient current of the faulty feeder can be expressed as

$$i_{n-T} = -(A_1 + L_p(C_{\Sigma} - C_n)(A_1 \delta^2 - A_1 \omega_f^2 - 2A_2 \omega_f \delta)) e^{-\delta t} \cos(\omega_f t) - (A_{124} + L_p(C_{\Sigma} - C_n)(A_2 \delta^2 - A_2 \omega_f^2 + 2A_1 \omega_f \delta)) e^{-\delta t} \sin(\omega_f t) \quad (8)$$

The transient current at the detection point $k(k=i+1, i+2, \dots, m)$ of the downstream of the fault point can be expressed as:

$$i_{Qk-T} = L_p \sum_{k=i+1}^m C_k (\delta^2 A_1 - A_1 \omega_f^2 - 2\delta A_2 \omega_f) e^{-\delta t} \cos(\omega_f t) + L_p \sum_{k=i+1}^m C_k (\delta^2 A_2 - A_2 \omega_f^2 + 2\delta A_1 \omega_f) e^{-\delta t} \sin(\omega_f t) \quad (9)$$

The transient current at the detection point $k(k=1, 2, \dots, i)$ of the upstream of the fault point can be expressed as:

$$i_{Qk-T} = L_p \left[\frac{(A_2 \omega_f - \delta A_1)}{R} + \sum_{k=i}^m C_k (\delta^2 A_1 - A_1 \omega_f^2 - 2\delta A_2 \omega_f) \right] e^{-\delta t} \cos(\omega_f t) + L_p \left[\frac{(-A_1 \omega_f - \delta A_2)}{R} + \sum_{k=i}^m C_k (\delta^2 A_2 - A_2 \omega_f^2 + 2\delta A_1 \omega_f) \right] e^{-\delta t} \sin(\omega_f t) \quad (10)$$

The transient currents at the fault point, each feeder, each detection point and transient voltage at the bus are all decaying sine component.

The transient current of a healthy feeder is proportional to derivative in the transient voltage of the bus. The transient current of a healthy feeder is approximately orthogonal to the transient voltage of the bus. The transient current of the faulty feeder consists of the transient current at the fault point and the transient capacitance ground current; the former is directly proportional (scale factor is the reciprocal of the fault resistance) to the magnitude of the transient voltage of the bus.

The transient current of a detection point on the downstream of the fault point is proportional to derivative in the transient voltage of the bus. The characteristics are the same with those of a healthy feeder. The transient current at the detection points which are on the upstream of the fault point comprise two parts, too. One part is the transient current at the fault point and the other is the sum of capacitive ground current of the downstream of each detection point. The characteristics are the same with those of faulty feeder.

Faulty feeder selection method of HIF

The healthy feeder's projection coefficient of the transient current with respect to transient voltage at the bus can be expressed as follows,

$$\xi_j = \frac{\langle i_{j-T}, u_{C-T} \rangle}{\|u_{C-T}\|^2} < 0 \quad (11)$$

The faulty feeder's projection coefficient can be expressed as follows,

$$\xi_n = \frac{\langle i_{n-T}, u_{C-T} \rangle}{\|u_{C-T}\|^2} = \frac{1}{R} + \frac{\langle i_{n-T}, u_{C-T} \rangle}{\|u_{C-T}\|^2} > 0 \quad (12)$$

From former section, it can be learnt that

$$\xi_n \gg \xi_j \quad (13)$$

the ξ_n has reverse polarity with ξ_j , and the magnitude of ξ_n is always larger than those of ξ_j and can be used to identify the faulty feeder.

By comparing each feeder's projection coefficient's magnitude and polarity, the feeder with the highest magnitudes and reverse polarity is the faulty feeder. If all the polarities of the projections are the same, it is a bus fault.

Location method of HIF

Similarly, by measuring the faulty feeder's transient current at each detection point and get their projection with respect to the transient voltage, the section's difference value γ_{cd} of transient current projection between the upstream detection point c and downstream detection point d can be calculated. The threshold value ρ_T is set at half of the maximum of each detection point's

projection coefficient. The section whose $\gamma_{cd} > \rho_T$ is the fault section. If no section satisfies this condition, the fault section is at the end of the feeder.

SYSTEM STRUCTURE ADAPTED TO HIF FEEDER IDENTIFICATION

System structure

The HIF identification system is composed of line selection device installed in the substation, feeder terminal unit (FTU) installed on feeder's each detection point, the master station installed on the control center and communication network. The main advantage is that: (1) It can determine the faulty feeders, improves the reliability of localization; (2) It can provide the fault information at outlet and eliminate blind area of location; (3) It can improve the anti-interference ability. The overall structure of the fault location system in distribution network is shown in Fig.2.

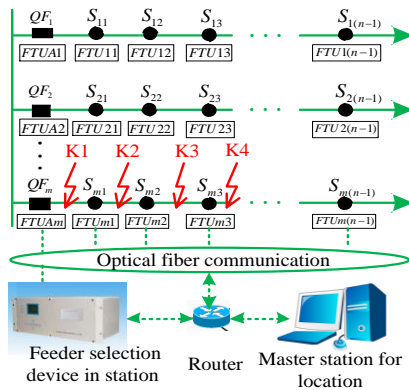


Fig. 2-Structure's diagram of faulty feeder identification system in distribution network

Process for faulty feeder identification

The implementation of the criterion is shown in Fig. 3.

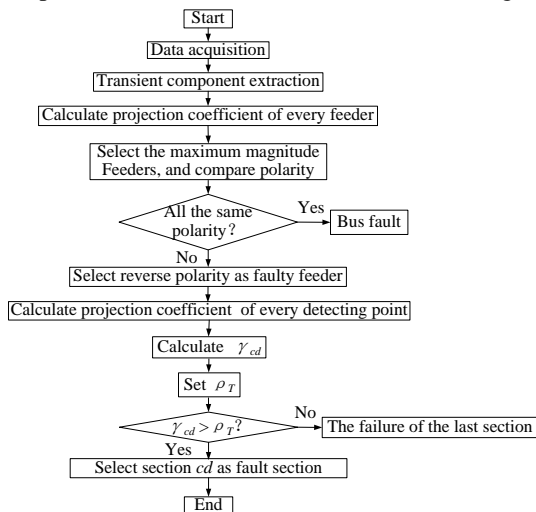


Fig. 3- Algorithm flowchart for faulty feeder identification

SIMULATION AND VERIFICATION USING FIDLD DATA

Verification of the simulation

The distributed parameter-based ATP simulation model for a typical 110 kV/10 kV distribution system is shown in Fig. 4. For a Petersen coil grounding network, the system is set to be over-compensated, with 108% compensation. The network comprises three mixed feeders with overhead lines and cables (feeders 1, 2 and 3) together with two cable feeders (feeders 4 and 5). HIFs occur in phase A of feeder 5.

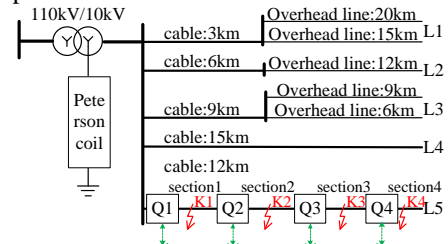


Fig. 4- Simulation model of a resonant grounding system. The waveforms of transient voltage of the bus, each feeder's transient current and their projection in the under-damping state in a distributed parameter model is shown in Fig.4, respectively, and feeder 5 is the faulty feeder. Assuming that under-damping ($R_f = 1500 \Omega$) fault occurred at K2 which is 7 km away from the bus on feeder 5, fault inception angle is 45° . To make the graphics more intuitive, only the typical waveforms of three feeders (faulty feeder and two healthy feeders) are drawn; the other two healthy feeders are proportional to feeders 1 and 4.

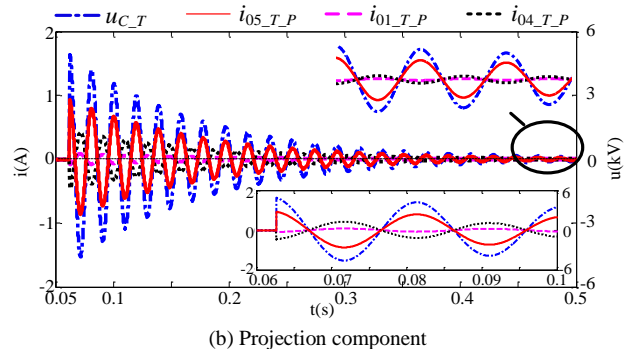
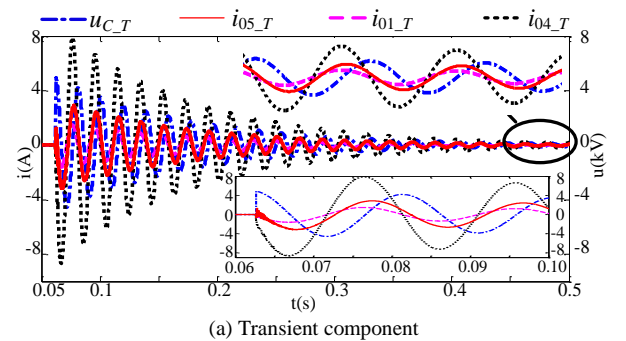


Fig. 5- Waveforms of each feeder current, voltage at the bus and their different components

The projection current into the healthy feeders is amplified in order to make the reverse polarity of the currents clear in Fig. 5 (b).

Table 1 shows the threshold value, the projection coefficient of each feeder and each detection point under different fault location, transition resistance, faulty inception angle and the selected faulty section in this condition.

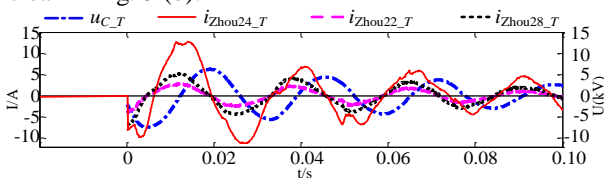
It can be learnt from the table 1 that, the magnitude of projection coefficient of healthy feeders and detection points on the downstream of the fault point is far less than that of faulty feeder and detections point on the upstream of the fault point. They share completely reverse polarity and have obvious fault characteristics.

Transition resistance/inception angle/fault location $\Omega^\circ/$	Threshold value ρ_T	Feeder's or detection point's projection coefficient				Fault feeder or section
		ζ_1	ζ_2	ζ_3	ζ_5	
		ζ_{Q1}	ζ_{Q2}	ζ_{Q3}	ζ_{Q4}	
1500/45/K2	-	-0.018	-0.033	-0.045	0.19	5
100/45/K2	4.239	8.089	8.479	-1.033	-0.516	2
100/45/K3	4.470	8.050	8.560	8.940	-0.510	3
100/90/K3	4.051	6.630	7.472	8.103	-0.842	3
1000/60/K4	0.525	0.811	0.900	0.965	1.051	4
1000/60/K1	0.415	0.830	-0.236	-0.171	-0.085	1
1000/90/K1	0.509	1.017	-0.101	-0.073	-0.036	1
3000/30/K2	0.065	0.119	0.129	-0.025	-0.012	2
3000/30/K1	0.060	0.119	-0.035	-0.025	-0.012	1
3000/90/K1	0.085	0.170	-0.002	-0.002	-0.001	1

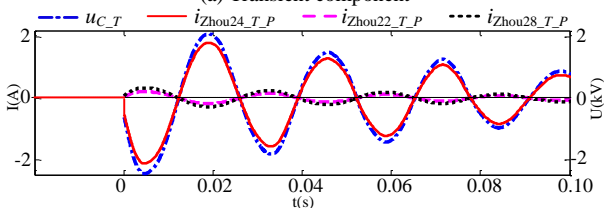
Table 1: The comparison of threshold value and the magnitude of transient current projection coefficient in every detecting point under different conditions

Verification of the field data

To verify the reliability of the method, we selected groups of field data, e.g., a group of field data from Zhoubang substation, Qingpu district, Shanghai, China in 2015. The system is 35/10 kV and the fault bus has 8 feeders. Feeder 'Zhou24' is the faulty feeder, and feeders 'Zhou 22' and 'Zhou 28' are healthy feeders with the highest relative current magnitudes. The projection current into the healthy feeders is amplified in order to make the reverse polarity of the currents clear in Fig. 5 (b).



(a) Transient component



(b) Projection component

Fig. 6- Waveforms of the field data

It can be learnt from the Fig.6(b) that, on the healthy feeder, the magnitude of transient current projection with respect to the transient voltage of the bus is far less than that of faulty feeder. They share completely reverse polarity and have obvious fault characteristics. It's consistent with the theoretical analysis, which can be used to select the faulty feeder.

CONCLUSIONS

For a resonant grounding system, the transient process of a HIF is the parallel resonance between the system capacitance to ground and the Petersen coil. By calculating and analyzing the transient current projection coefficient of each feeder and detection point with respect to the transient voltage, it can be learnt that the magnitude of transient current projection coefficient of healthy feeders is far less than that of faulty feeder. They share completely reverse polarity. It can also be learnt that the magnitude of transient current projection of detection point on the downstream of the fault point is far less than that of detection point on the upstream of the fault point. They share completely reverse polarity, too. According to the difference of magnitude and polarity, detection method for HIF is put forward. The schematic diagram of system results and the flow chart of algorithm are provided.

REFERENCES

- [1] M. Aucoin., Mar, 1985, "Status of high impedance fault detection," IEEE Trans. Power App. Syst., vol. PER-5, no. 3, pp. 39-40.
- [2] Griffel D, Harmmand Y, Oct. 1997, "A new deal for safety and quality on MV networks," IEEE Trans. Power Del., vol. 12, no. 4, pp. 1428-1433.
- [3] H. Ma, X. Zeng, Y. Wang, Z. Li, Aug. 2005, "Grounding fault protection with fault resistance measuring for ineffectively earthed power systems," in Proc. IEEE/PES Transmission and Distribution Conference & Exhibition, pp. 1-3.
- [4] T. Welfonder, V. Leitloff, R. Fenillet, S. Vitet, Oct. 2000, "Location strategies and evaluation of detection algorithms for earth faults in compensated MV distribution systems" IEEE Trans. Power Del., vol. 15, no. 4, pp. 1121-1128.
- [5] G. Druml, W. Klein, O. Seifert, 2009, "New adaptive algorithm for detecting low- and high ohmic faults in meshed networks," in Proc. CIRED.
- [6] G. Druml, A. Kugi, O. Seifert, 2003, "A New Directional Transient Relay for High Ohmic Earth Faults," in Proc. CIRED.
- [7] D. Xue, J. LI, Y. XU, 2013, "Transient equivalent circuit of single-phase earth faults on isolated neutral system," in Proc. CIRED.